

# Uniform Field in Microwave Cavities Through the Use of Effective Magnetic Walls

Jim A. Enriquez\*

*Physics Department, National University of Colombia, 111321, Bogota, Colombia*

Rustam Balafendiev\*

*Science Institute, University of Iceland, Dunhagi 5, 107 Reykjavik, Iceland*

Alexander J. Millar

*Theoretical Physics Division, Fermi National Accelerator Laboratory, Batavia, IL 60510, USA and  
 Superconducting Quantum Materials and Systems Center (SQMS),  
 Fermi National Accelerator Laboratory, Batavia, IL 60510, USA*

Constantin Simovski

*Department of Electronics and Nanoengineering, Aalto University, Maarintie 8, FI00076, Espoo, Finland*

Pavel Belov

*Qingdao Innovation and Development Center, Harbin Engineering University, Qingdao 266000, Shandong, China and  
 School of Engineering, New Uzbekistan University,  
 Movarounnahr str. 1, 100000, Tashkent, Uzbekistan*

(Dated: December 4, 2024)

Wire media (WM) resonators have emerged as promising realization for plasma haloscopes – devices designed to detect axions, a potential component of dark matter. Key factors influencing the detection probability include cavity volume, resonance quality factor, and form factor. While the form factor has been explored for resonant frequency tuning, its optimization for axion detection remains unexplored. In this work, we present a novel approach to significantly enhance the form factor of WM plasma haloscopes. By shifting the metal walls of the resonator by a quarter wavelength, we effectively convert an electric wall boundary condition into a magnetic wall one, allowing for an almost uniform mode. Theoretical analysis and numerical simulations confirm that this modification improves the electric field profile and boosts the form factor. We validate these findings through experimental results from two prototype resonators: one with a standard geometry and another with a quarter-wave air gap between the WM and the walls. Additionally, our method provides a simple way to control the field profile within WM cavities, which can be explored for further applications.

## I. INTRODUCTION

Wire media (WM), initially proposed by Brown [1] and Rotman [2], and later studied by Pendry and Belov et al. in works [3, 4], have garnered significant attention for their distinctive properties as an artificial plasma material. These structures, comprising a dense array of parallel metallic wires embedded in a dielectric host, exhibit a tunable plasma frequency that can be adjusted by modifying their geometrical parameters. Beyond theoretical exploration, WM-based devices have found practical applications in diverse fields, ranging from microwave antennas [5] to near-field thermophotovoltaic systems [6] and systems of radiative cooling [7]. A detailed review about WM applications can be found in Ref. [8].

Previous investigations into WM open resonators have primarily focused on exploiting topological transitions in their isofrequency contours to achieve a notable Purcell factor [9, 10]. More recently, cavities consisting in WM enclosed by metallic walls and placed in a DC magnetic

field, often referred to as plasma haloscopes [11], have emerged as a promising technique for the detection of axions, a possible candidate for dark matter [12]. One can also look for dark photons, another promising dark matter candidate even if the magnetic field is absent [13]. Our earlier studies of WM-filled cavities demonstrated that WM operating in the epsilon-near-zero (ENZ) regime significantly extends the wavelength of light within the medium, resulting in a low-frequency fundamental resonance and a high degree of field uniformity [14].

The improvement of field homogeneity in microwave resonators have been studied in the context of electron paramagnetic resonance (EPR), where axially uniform field distribution for a TE mode is a desirable feature [15]. A common approach to higher uniformity of the field pattern in hollow metal cavities involves a design with a central region surrounded by two end regions. The central region functions as a metallic waveguide operating at its cutoff frequency, while the optical length of the end regions is set to a quarter of a wavelength [15]. Various configurations for end regions in hollow metal cavities have been proposed, including dielectric rods with the same cross-section as the central region [16], modified

\* These authors contributed equally.

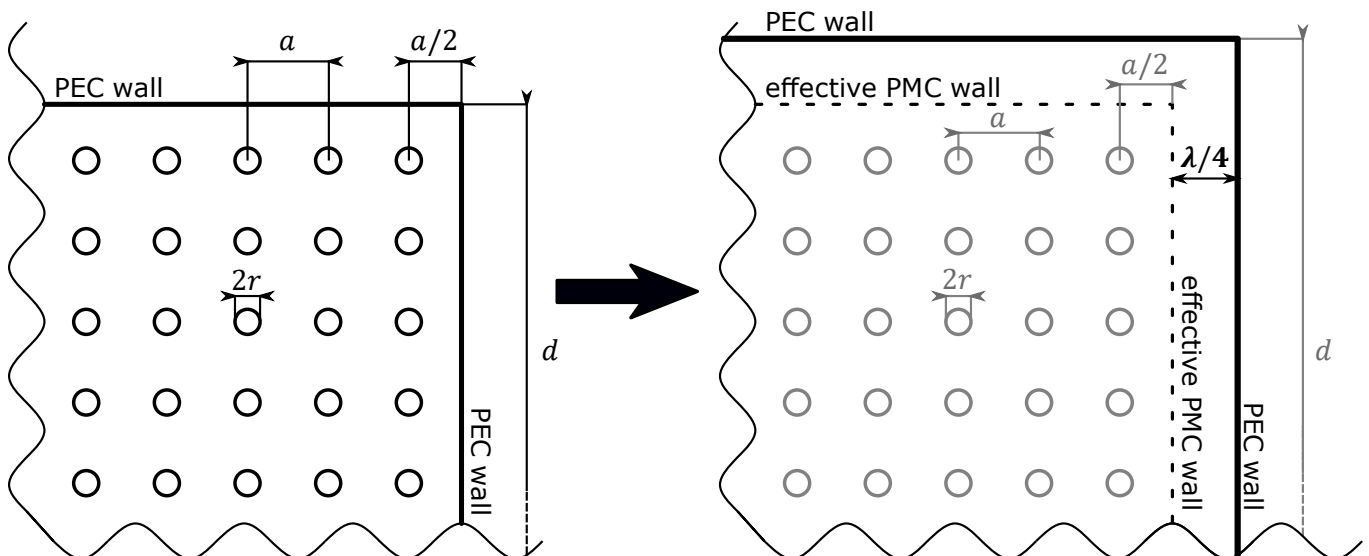


FIG. 1: Schematic representation of the proposed modification to the cavity's boundary condition. A wire medium (WM) resonator consists on an arrange of metallic wires with radius  $r$ , distributed with a period  $a$ . In a regular configuration, the distance between the last set of wires and the cavity walls, made of perfect electric conductor (PEC), is  $a/2$ . By adjusting this distance to  $a/2 + \lambda/4$ , the boundary enclosing the WM behaves effectively as a perfect magnetic conductor (PMC) wall.

cross sections larger than that of the central region [17], and conducting rods insertions [18].

As to the axion haloscopes, the field uniformity is just as beneficial for them as for EPR devices. Several key characteristics should be engineered to enhance their performance: the strength of the DC magnetic field, cavity volume, quality factor, and form factor are critical factors influencing the power from photon-axion conversion in resonance [19]. The form factor for a mode in a plasma haloscope, characterized by an electric field  $\mathbf{E}_{lmn}$ , is defined as

$$C_{lmn} = \frac{|\iint_V \mathbf{B}_0 \cdot \mathbf{E}_{lmn} dV|^2}{V B_0^2 \iint_V \epsilon |\mathbf{E}_{lmn}|^2 dV}, \quad (1)$$

where  $V$  is the cavity volume,  $\epsilon$  is the relative permittivity within the cavity, and  $\mathbf{B}_0$  is the external DC magnetic field, which we will take to be spatially constant and aligned with the wires.

To ensure the highest field homogeneity inside plasma haloscopes, and thus the optimal form factor, the focus has been on the study of the fundamental TM cavity mode [20–23]. The fundamental TM mode in a WM resonator, with WM as the cavity content, exhibits a uniform axial field profile and a sinusoidal transverse pattern due to the electric wall boundary conditions and the axial polarization of the electric field [14]. In wedge-shaped haloscopes, the quarter-wavelength long corrugations of the walls were utilized to achieve the field uniformity in the axial direction [24, 25]. Meanwhile, improving field homogeneity in WM resonators along the transversal section remains an unexplored area.

In this work we show that placing the walls with the

quarter-wavelength gap from the WM interface, we effectively transform this interface from the perfect electric conductor (PEC) into a perfect magnetic conductor (PMC). Figure 1 illustrates this concept. This transformation is similar to the conversion of a shortened transmission line into an open one by shifting the termination by an odd number of quarter-wavelengths. By modifying the boundary conditions, we create a cavity whose fundamental mode is  $TM_{000}$  rather than the  $TM_{110}$  mode of the regular cavity. This transition significantly improves the form factor and shifts the fundamental resonance frequency down to the plasma frequency.

To investigate the enhancement of form factor in wire medium (WM) resonators, we propose an analytical model taking into account the boundary conditions at the WM interfaces separated from the cavity walls by arbitrary air gaps. Using this model, we estimate the resonance frequency and form factor of square transverse section WM cavities. We compare the analytical results with numerical simulations and present experimental and full-wave simulation data for the spectra and form factors of two WM resonator prototypes fabricated using printed circuit boards (PCBs). Our findings demonstrate a significant increase in the form factor when introducing an air gap with an optimal thickness, close to a quarter of the resonant wavelength, between the WM and the cavity walls.

## II. ANALYTICS

### A. Effective boundary condition

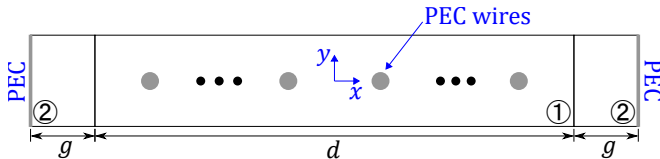


FIG. 2: One-dimensional schematic of a resonator composed of a wire medium (region 1) with thickness  $d$  surrounded by an air gap (region 2) with thickness  $g$ .

To assess the impact of the air gap between the wall and the WM on the modal field uniformity, we develop a one-dimensional analytical model. We focus on the TM modes because the TE modes weakly interact with the WM. We divide the system into two regions, as depicted in Fig. 2. Region 1 contains the lossless (PEC wires) WM characterized by a relative permittivity [8]

$$\epsilon = 1 - \left(\frac{k_p}{k_0}\right)^2, \quad (2)$$

where  $k_0$  is the vacuum wave number and  $k_p = \frac{2\pi}{\lambda_p}$ , with  $\lambda_p$  being the plasma wavelength. Region 2 represents the air gap between the WM and the PEC walls. Horizontal lines in Fig. 2 outline a unit cell of the infinitely extended parallel-plate cavity. By imposing the inherent odd symmetry of the electric field and even symmetry of the magnetic field due to the PECs, we derive the TM mode solutions to Maxwell's equations as follows:

$$E_z(x) = \begin{cases} A \cos(k_{x1}x) & |x| \leq \frac{d}{2} \\ B \sin(k_{x2}(\frac{d}{2} + g - |x|)) & |x| > \frac{d}{2} \end{cases}, \quad (3)$$

$$H_y(x) = \begin{cases} -jA \frac{k_{x1}}{\eta_0 k_0} \sin(k_{x1}x) & |x| \leq \frac{d}{2} \\ -j \frac{x}{|x|} B \frac{k_{x2}}{\eta_0 k_0} \cos(k_{x2}(\frac{d}{2} + g - |x|)) & |x| > \frac{d}{2} \end{cases}, \quad (4)$$

where  $k_{x1} = \sqrt{\epsilon}k_0$ , and  $k_{x2} = k_0$ , assuming no field dependence on  $x$  and  $z$ . We evaluate the field solutions in Eqs. (3) and (4) at  $x = \frac{d}{2}^+$  (on the side of the air gap) to derive a surface impedance that represents the effective boundary condition for the WM interface,

$$Z = \frac{|E_z|(\frac{d}{2}^+)}{|H_y|(\frac{d}{2}^+)} = \frac{\eta_0 k_0 \sin(k_{x2}g)}{k_{x2} \cos(k_{x2}g)}. \quad (5)$$

This impedance vanishes for  $g = 0$ , corresponding to a perfect electric conductor, and approaches infinity as  $g$  tends to  $\lambda/4$  matching the wave impedance of a perfect magnetic conductor.

### B. Fundamental mode of WM resonator

In this section, we investigate the TM modes of a 1D WM resonator illustrated by Fig. 2 for the limit cases of  $g = 0$  and  $g = \lambda/4$ . We assume no field variation along the  $z$ -axis for the fundamental WM resonator mode (i.e.  $k_z = 0$ ) and consider a square resonator cross-section (implying  $k_x = k_y = k_{t1}$ ). Using these assumptions, we express the electromagnetic field within the effective WM as

$$\left. \begin{aligned} E_z &= E_0 \cos(k_{t1}x) \cos(k_{t1}y) \\ H_x &= jE_0 \frac{k_{t1}}{\eta_0 k_0} \cos(k_{t1}x) \sin(k_{t1}y) \\ H_y &= -jE_0 \frac{k_{t1}}{\eta_0 k_0} \sin(k_{t1}x) \cos(k_{t1}y) \end{aligned} \right\} |x|, |y| \leq \frac{d}{2}. \quad (6)$$

For the fundamental TM mode within the effective WM region, defined by  $|x|, |y| \leq \frac{d}{2}$ , we define the wave number as

$$\epsilon k_0^2 = k_x^2 + k_y^2 = 2k_{t1}^2, \quad (7)$$

while we define the wave number in the air gap region, for instance where  $x > \frac{d}{2}, |y| \leq \frac{d}{2}$ , as

$$k_0^2 = k_{x1}^2 + k_{y2}^2 = k_{t1}^2 + k_{t2}^2. \quad (8)$$

Utilizing Eqs. (7) and (8), and solving for  $k_{t1}$  and  $k_{t2}$ ,

$$\left. \begin{aligned} k_{t1}^2 &= \frac{\epsilon}{2} k_0^2, \\ k_{t2}^2 &= \left(1 - \frac{\epsilon}{2}\right) k_0^2. \end{aligned} \right\} \quad (9)$$

It is important to note that in this model, the WM resonator has no corners, which may have impact for the real resonator. Despite this approximation, we can employ the one-dimensional solution to estimate the two-dimensional behavior, analogous to Marcattili's method for dielectric rectangular waveguides [26]. This approximation is valid when the field is primarily concentrated in the central region.

Matching the surface wave impedance of the field at the effective WM boundary (Eqs. (6)) with that of the effective boundary condition (Eq. (5)), particularly at  $x = \frac{d}{2}, |y| \leq \frac{d}{2}$ , we derive the following dispersion equation:

$$k_{t1} \tan(k_{t1} \frac{d}{2}) - k_{t2} \cot(k_{t2}g) = 0. \quad (10)$$

This dispersion equation yields the resonance frequencies of the TM modes. Notably, using Eq. (9), we can determine the resonance frequency of the fundamental TM mode. For the fundamental mode, when  $g = \lambda/4$ , the second term in Eq. (10) vanishes, implying that  $k_{t1} = 0$ . Consequently,  $\epsilon = 0$  and  $k_0 = k_p$ , leading to a constant electric field according to Eq. (6). It is worth mentioning that Eq. (10) is similar to the dispersion equation

derived in Ref. [16]. However, while Ref. [16] achieves field homogeneity in a single direction by using a central metallic waveguide operating at its cutoff frequency, our approach requires a WM in the central region of the cavity operating at the plasma frequency to ensure field homogeneity in both transverse directions.

In order to quantify the field uniformity in the WM resonator, we use a 2D version of the form factor in Eq. (1),

$$C = \frac{(\iint_S E_z dS)^2}{S \iint_S |\mathbf{E}|^2 dS}, \quad (11)$$

where  $S$  is the area of the transversal section of the 2D WM resonator,  $(d + 2g) \times (d + 2g)$ .

### C. Results

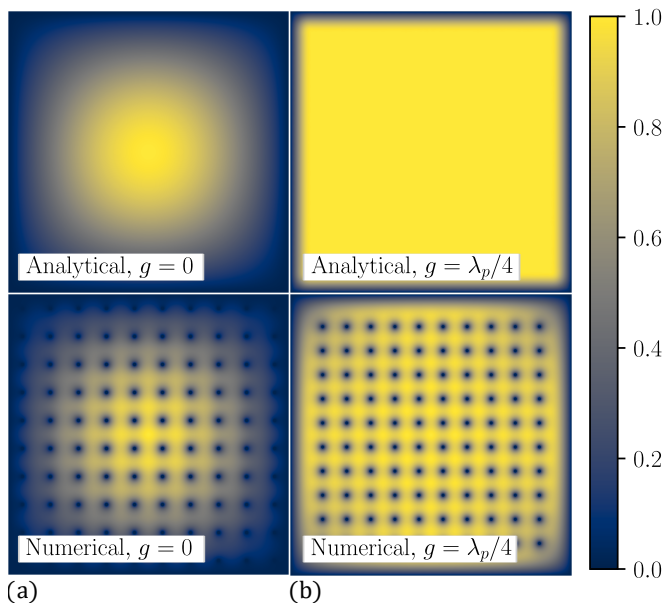


FIG. 3: Electric field distribution in a wire medium (WM) resonator: (a) Regular WM resonator with no air gap ( $g = 0$ ), and (b) WM resonator with an air gap of thickness  $g = \lambda_p/4$ . The introduction of the air gap ( $g = \lambda_p/4$ ) results in a more uniform electric field distribution.

We used full-wave simulations in a COMSOL Multiphysics eigenmode solver to validate the applicability of our 1D theory to a 2D cavity. In both our analytical calculations and simulations, the cavity comprised an array of  $10 \times 10$  infinitely long wires with wire radius  $r_0 = 0.5$  mm and inter-wire spacing  $a = 10$  mm. We adopted the generalized quasi-static approach from Ref. [27] to determine the requisite plasma frequency for the theoretical model.

Figure 3 illustrates the arbitrary normalized electric field distribution for the fundamental TM mode over the transverse ( $xy$ ) plane of the cavity for two specific cases:

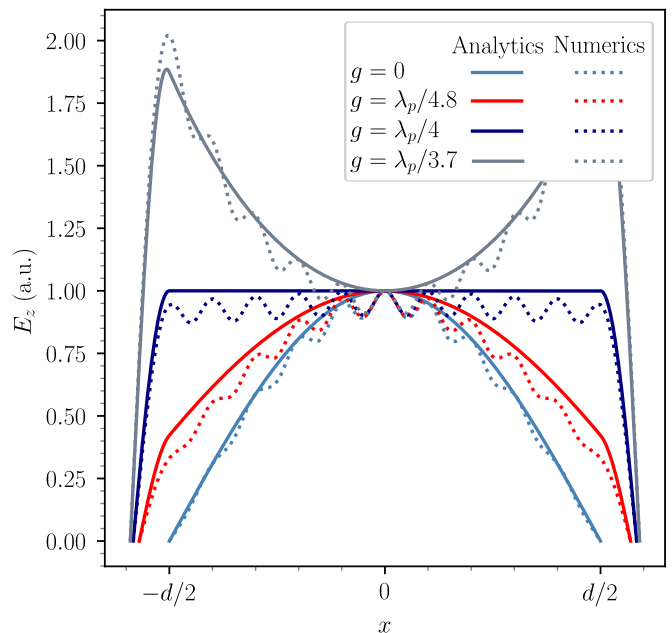


FIG. 4: Wire medium (WM) resonator electric field profile for different air gap thicknesses,  $g$ . The WM extends from  $x = -\frac{d}{2}$  to  $x = \frac{d}{2}$ . A uniform electric field in the WM region is observed at  $g = \lambda_p/4$ .

$g = 0$  and  $g = \lambda_p/4$ . Our numerical and analytical findings confirm that introducing a  $\lambda_p/4$  air gap homogenizes the electric field distribution in a finite-cross section sample of the WM.

The electric field profile along the  $x$ -axis for the fundamental TM mode of a WM resonator varies with the gap width,  $g$ , as shown in Fig. 4. The electric field homogeneity improves with increasing  $g$  until reaching a maximum at  $g = \lambda_p/4$ . Introducing a quarter-wavelength air gap between the effective wire medium and the PEC walls significantly flattens the electric field profile, confining the field decay primarily to the newly added  $\lambda_p/4$  region. This coincides with a pronounced magnetic field enhancement within the same gap, offering potential for readout applications. For the gap exceeding  $\lambda_p/4$ , the field concentrates near the resonator walls, and the underlying assumption of field confinement within the wire medium becomes not adequate.

Figure 5 illustrates the resonant frequency (Fig. 5a) and form factor (Fig. 5b) of the fundamental mode in such WM resonator as a function of the air gap,  $g$ . The resonant frequency remains nearly constant for  $0 \leq g \leq \lambda_p/4$ , aligning with the plasma frequency at  $g = \lambda_p/4$ . Conversely, the form factor progressively increases, reaching a maximum at an air gap of approximately  $g = \lambda_p/4$ . While the resonant frequency exhibits excellent agreement between analytical and numerical results, coming from both a physical WM and an effective WM, within this range, a slight discrepancy arises in the form factor. This error results from the evident difference between the effective and physical (real) WM. In



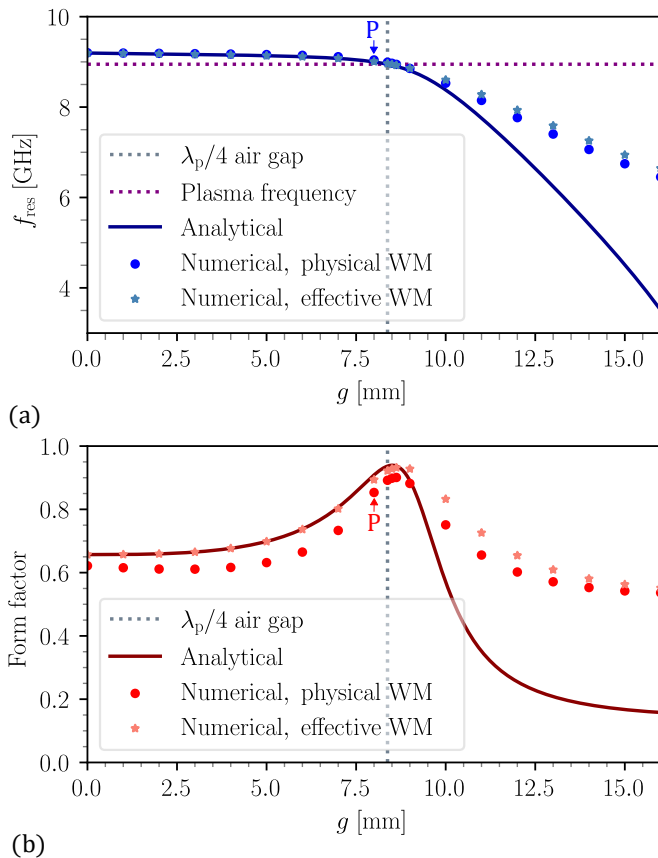


FIG. 5: Characteristics of wire medium (WM) resonator fundamental TM mode. a) Resonance frequency and b) form factor for different air gap thicknesses,  $g$ . A form factor of approximately 0.92 is observed at  $g = \lambda_p/4$  for an effective WM (theory and numerics) while a form factor of 0.89 is observed for the physical WM (numerics). Point P corresponds to the air gap thickness used in the experimental section.

the effective-medium model there are no wires and the field does not vanish inside this medium, whereas in the physical WM it vanishes within every wire – see the dark spots in the bottom panel of Fig. 3b. In accordance with numerical calculations of the mode field within a single unit cell of our WM the maximally achievable form factor corresponding at 8.9 GHz to  $g = \lambda_p/4 = 8.4$  mm is equal to 0.92, as well as in the analytical model. However, the simulation of the physical WM corresponding to the bottom panel of Fig. 3b shows the form factor 0.89. Despite this, the maximum form factor occurs at nearly the same air gap value in both numerical simulations and the analytical model. For smaller gaps the agreement between the analytical and numerical results corresponding to physical WM is good, and is excellent for the numerical simulations of the effective WM sample surrounded by the PEC walls. Thus, these results fully justify the model of an effective WM sample for  $g \leq \lambda_p/4$ . For  $g > \lambda_p/4$ , the agreement between the analytical model

and numerical simulations disappears due to the effect of the field concentration in the air gap. This effect invalidates the initial assumption of field confinement within the WM sample. However, the agreement between the results obtained for the effective WM sample and for the array of separate wires keeps.

It is evident that the maximal form factor corresponds to the perfect magnetic wall effectively located on the WM-air interface. The PEC wall shifts the phase of a reflected wave by  $\pi$ , the air gap grants an extra  $\pi$ , so the phase of the reflected wave does not change. Therefore, the mode inside the WM sample is the standing wave shaped by four perfect magnetic boundaries surrounding the sample. Note that this effective boundary condition can be achieved through various methods that introduce an extra phase shift of  $\pi$  between incident and reflected waves, as detailed in [16–18]. This flexibility may help the  $\text{TM}_{000}$  modes implementation in innovative plasma haloscope designs that require tunability.

### III. EXPERIMENT

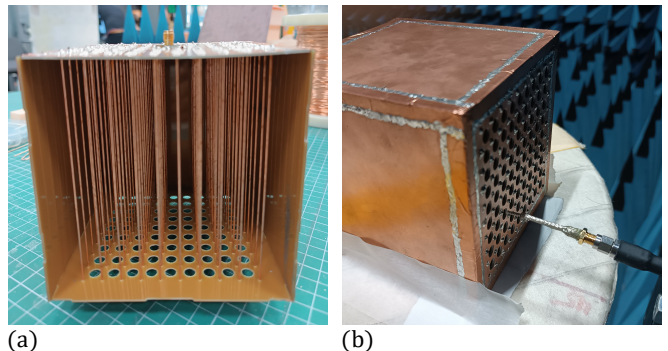


FIG. 6: Prototype WM resonators with different wall spacing. The resonators consist of  $10 \times 10$  arrays of copper wires with a period of  $a = 1$  cm. The first resonator is a regular resonator with a distance of  $a/2$  between the wires at the edge and the walls, and the second one is  $\lambda/4.2$ -shifted with a distance of approximately  $a/2 + \lambda/4.2$  between the wires at the edge and the walls. (a) Unfinished state of the regular resonator. Copper wires (radius 0.5 mm) are inserted into the FR-4 PCB walls with a period of 1 cm. (b) Finished prototype being scanned through pre-drilled holes by a movable antenna.

We fabricated two prototypes to validate the claimed effect. The first prototype represents the regular (conventional) configuration, see for example Ref. [14], where the air gap between the array of wires and the cavity walls is equal  $a/2$ . The second prototype incorporates a configuration we specially optimized for the cubic resonator to enhance field homogeneity and to avoid situations where the air gap exceeds  $\lambda_p/4$ , as this would lead the field to localize mainly near the cavity walls (see Fig. 4). In this

3D case, the designed gap is slightly smaller than the quarter-wavelength. So, for the optimized resonator, the edge wires of the array are distanced from the walls by  $(a/2 + \lambda_p/4.2)$ . For the 2D resonator, this configuration would correspond to point P in Fig. 5. Below we call our optimized cubic resonator the  $\lambda_p/4.2$ -shifted one.

We fabricated the prototype enclosures using single-sided metal FR-4 PCBs of 1 mm thickness. We arranged these PCBs into cubes with dimensions of 10 cm x 10 cm x 10 cm for the regular resonator and 11.6 cm x 11.6 cm x 11.6 cm for the  $\lambda/4.2$ -shifted resonator. To complete the resonators, we inserted and welded one hundred copper wires, each with a radius of 0.5 mm, into the PCB cubes with a periodic spacing of  $a = 1$  cm, as shown in Fig. 6a.

We equipped each resonator prototype with a 4-mm long SMA connector attached to its bottom plate for signal feeding. The SMA port functions similarly to a monopole antenna, exciting the TM modes within the resonator cavity. To characterize the electric field distribution of the TM modes, we positioned a separate monopole antenna through a pre-drilled array of holes on the top plate of each resonator, as illustrated Fig. 6b. This monopole antenna was a coaxial cable with a center conductor radius of 0.25 mm, extending 4 mm into the resonators through the holes. The hole array comprised 81 individual holes, arranged in a square grid with a period of  $a = 1$  cm and a hole radius of  $r_h = 3$  mm.

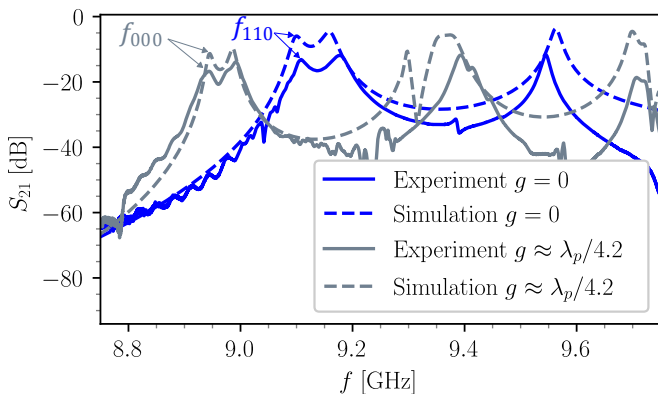


FIG. 7: Experimentally measured  $S_{21}$  parameter for wire media resonators: (a) Regular resonator and (b)  $\lambda_p/4.2$ -shifted resonator. Measurements were performed by placing the movable monopole antenna in the central hole. The resonance frequency of the fundamental TM mode in the regular resonator ( $f_{110}$ ) is 9.11 GHz (experiment) and 9.10 GHz (simulation), while in the  $\lambda_p/4.2$ -shifted resonator ( $f_{000}$ ) it is 8.943 GHz (experiment and simulation).

We measured the S-parameters using a Rohde & Schwarz ZVB20 vector network analyzer (VNA) across a frequency range of 8.75-9.75 GHz. The fixed antenna, located on the bottom plate of each prototype, was connected to one port of the VNA, while the movable antenna on the top plate was connected to the other port. To measure the  $S_{21}$ , we positioned the monopole antenna

in the array of holes. Fig. 7 displays the measured  $S_{21}$  when the movable antenna was placed in the central hole of each prototype. We observe that the spectrum of the  $\lambda_p/4.2$ -shifted resonator is red-shifted relative to that of the regular resonator, as predicted by theory for the fundamental mode. Meanwhile, the amplitude levels and shape of the spectrum change slightly, indicating that the quality factor of the resonator is not significantly affected when an air gap of  $\lambda_p/4.2$  is introduced.

We conducted full-wave simulations of cubic resonators, corresponding to the experimental prototypes, using CST Studio. Copper was modeled with a conductivity of  $\sigma = 5.7 \times 10^7$  S/m, while the FR-4 layers of the PCBs were represented as lossy dielectrics with a dielectric constant of  $\epsilon = 4.3$  and a loss tangent of  $\tan \delta = 0.025$ . We measured the  $S_{21}$  parameter and positioned a field monitor at the first resonance frequency for each resonator.

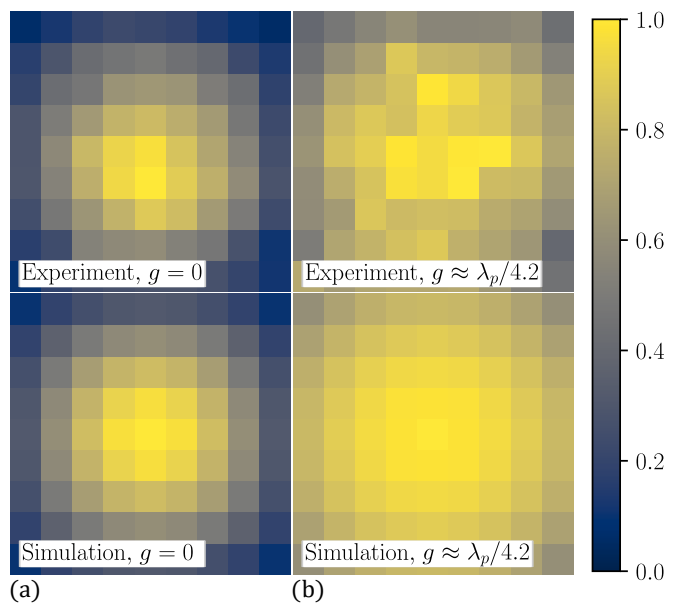


FIG. 8: Measured electric field distribution of the fundamental TM mode in wire media resonators: (a) Regular resonator and (b)  $\lambda/4.2$ -shifted resonator. Pixel intensities represent the magnitude of the  $S_{21}$  parameter measured at the fundamental resonance frequencies,  $f_{110}$  and  $f_{000}$  (marked in Fig. 7), through pre-drilled holes at one end of the cavities.

We characterized the operation of the two resonators under comparison by examining the first peaks of the  $S_{21}$ -parameter spectra. These peaks correspond to the  $TM_{110}$  mode for the regular resonator and the quasi- $TM_{000}$  mode for the  $\lambda_p/4.2$ -shifted resonator, as shown in Fig. 7. We do not consider high-order modes, as they are not relevant for our purpose of achieving the highest field homogeneity (see e.g. in Refs. [14, 17]). Fig. 8 presents the measured electric field distributions for both prototypes at the corresponding frequencies ( $f_{000}$  for the  $\lambda_p/4.2$ -shifted resonator and  $f_{110}$  for the regular one).

We observe a significant improvement in field homogeneity for the  $\lambda_p/4.2$ -shifted resonator compared to the regular resonator. This observation is further supported by the measured form factors, with a value of 0.77 (experiment), 0.80 (simulation) for the  $\lambda_p/4.2$ -shifted resonator compared to 0.61 (experiment), 0.64 (simulation) for the regular resonator.

So, our experimental results demonstrate an improvement in field homogeneity due to the optimized gap between the WM sample and the resonator walls. Slight discrepancies between experimental and simulation results seen in the field maps of Fig. 8 can be attributed to experimental limitations in the prototype fabrication and the field scanning procedure. Due to manual soldering of the wires, variations in wire length within the prototypes may exist. Additionally, excessive heat during soldering could have caused material deformations, leading to bending in either the wires or PCB plates. Moreover, the scanning procedure, involving the antenna traversing through holes, might have introduced slight variations in field measurements if the antenna was not perfectly centered at each hole. This could explain the difficulty in differentiating between high field levels and the exact location of the maximum field, which was not precisely at the central hole as simulations predicted.

#### IV. CONCLUSIONS

We introduced a new method to enhance field homogeneity within WM resonators. Our theoretical model, supported by numerical simulations, demonstrated that properly increasing the air gap between the resonator walls and the WM sample, one can effectively manipulate the field homogeneity. When the air gap reached one-quarter of the resonant wavelength, the field homogeneity peaked, theoretically resulting in a form factor of 0.92 for an effective WM model (theory and simulations) and 0.89 for a physical array of wires (simulations). Additionally, this enhancement in the form factor was accompanied by a shift in the resonant mode frequency toward the plasma frequency.

We experimentally validated the proposed method by developing two prototype resonators: a regular WM

resonator containing the WM sample with the conventional half-period air gap between the wires and the walls and an optimized  $\lambda_p/4.2$ -shifted resonator. We devised a method to measure the field distribution within the transverse section of the cavities, enabling the subsequent calculation of the form factor. This method involved measuring the magnitude of the  $S_{21}$  parameter using a fixed antenna at one end of the resonator and a scanning antenna at the other end. The scanning antenna traversed predrilled holes within the resonator. Comparing experimental results with full-wave simulations, we found that the form factor in a standard WM resonator was 0.61 (experiment) and 0.64 (simulation), whereas in the approximately  $\lambda/4.2$ -shifted WM resonator, the form factor increased to 0.77 (experiment) and 0.80 (simulation). Our findings validate and substantiate using the  $TM_{000}$  mode to improve the form factor in plasma haloscopes, opening new avenues for WM cavity applications where precise control of the internal field profile is essential.

In order to realize a practical experiment, there are two main avenues for future work. The first is to adapt the cavity design to have a cross-section better suited for a cylindrical bore of a solenoidal magnet. Secondly, given purpose of the plasma haloscopes inherently requires their resonance frequency to be tunable in order to search for dark matter at different frequencies, we plan to investigate the effectiveness of the proposed approach in improving the form factor when the mode frequency varies. This will involve considering both operation away from the quarter-wave condition and adjustment of the walls to maintain it, similarly to the tuneable rectangular cavity in Ref. [28].

#### ACKNOWLEDGEMENTS

The authors thank Eugene Koreshin for helpful discussions and also thank the members of the ALPHA Consortium for discussion and support.

Fermilab is operated by the Fermi Research Alliance, LLC under Contract DE-AC02-07CH11359 with the U.S. Department of Energy.

- 
- [1] J. Brown, Artificial dielectrics, *Progress in Dielectrics* **2**, 195 (1960).
  - [2] W. Rotman, Plasma simulation by artificial dielectrics and parallel-plate media, *IEEE Trans. Antennas Propag.* **3**, 82 (1962).
  - [3] J. B. Pendry, A. J. Holden, D. J. Robbins, and W. J. Stewart, Low frequency plasmons in thin-wire structures, *J. Condens. Matter Phys.* **10**, 4785 (1998).
  - [4] P. A. Belov, R. Marqués, S. I. Maslovski, I. S. Nefedov, M. Silveirinha, C. R. Simovski, and S. A. Tretyakov, Strong spatial dispersion in wire media in the very large wavelength limit, *Phys. Rev. B* **67**, 113103 (2003).
  - [5] E. Forati, G. W. Hanson, and D. F. Sievenpiper, An Epsilon-Near-Zero Total-Internal-Reflection Metamaterial Antenna, *IEEE Trans. Antennas Propag.* **63**, 1909 (2015).
  - [6] C. Simovski, S. Maslovski, I. Nefedov, and S. Tretyakov, Optimization of radiative heat transfer in hyperbolic metamaterials for thermophotovoltaic applications, *Opt. Express* **21**, 14988 (2013).
  - [7] C. Simovski, S. Maslovski, I. Nefedov, S. Kosulnikov, P. Belov, and S. Tretyakov, Hyperlens makes thermal

- emission strongly super-Planckian, *Photonics Nanostructures: Fundam. Appl.* **13**, 31 (2015).
- [8] C. R. Simovski, P. A. Belov, A. V. Atrashchenko, and Y. S. Kivshar, Wire metamaterials: physics and applications, *Adv. Mater.* **24**, 4229 (2012).
- [9] M. S. Mirmoosa, S. Y. Kosulnikov, and C. R. Simovski, Magnetic hyperbolic metamaterial of high-index nanowires, *Phys. Rev. B* **94**, 075138 (2016).
- [10] M. S. Mirmoosa, S. Y. Kosulnikov, and C. R. Simovski, Double resonant wideband Purcell effect in wire metamaterials, *J. Opt.* **18**, 095101 (2016).
- [11] M. Lawson, A. J. Millar, M. Pancaldi, E. Vitagliano, and F. Wilczek, Tunable Axion Plasma Haloscopes, *Phys. Rev. Lett.* **123**, 141802 (2019).
- [12] A. J. Millar, S. M. Anlage, R. Balafendiev, P. Belov, K. van Bibber, J. Conrad, M. Demarteau, A. Droster, K. Dunne, A. G. Rosso, J. E. Gudmundsson, H. Jackson, G. Kaur, T. Klaesson, N. Kowitz, M. Lawson, A. Leder, A. Miyazaki, S. Morampudi, H. V. Peiris, H. S. Røising, G. Singh, D. Sun, J. H. Thomas, F. Wilczek, S. Withington, M. Wooten, J. Dilling, M. Febraro, S. Knirck, and C. Marvinney (Endorsers), Searching for dark matter with plasma haloscopes, *Phys. Rev. D* **107**, 055013 (2023).
- [13] G. B. Gelmini, A. J. Millar, V. Takhistov, and E. Vitagliano, Probing dark photons with plasma haloscopes, *Phys. Rev. D* **102**, 043003 (2020), [arXiv:2006.06836 \[hep-ph\]](https://arxiv.org/abs/2006.06836).
- [14] R. Balafendiev, C. Simovski, A. J. Millar, and P. Belov, Wire metamaterial filled metallic resonators, *Phys. Rev. B* **106**, 75106 (2022).
- [15] J. S. Hyde, J. W. Sidabras, and R. R. Mett, Uniform Field Resonators for EPR Spectroscopy: A Review, *Cell Biochem. Biophys.* **77**, 3 (2019).
- [16] R. R. Mett, W. Froncisz, and J. S. Hyde, Axially uniform resonant cavity modes for potential use in electron paramagnetic resonance spectroscopy, *Rev. Sci. Instrum.* **72**, 4188 (2001).
- [17] J. R. Anderson, R. R. Mett, and J. S. Hyde, Cavities with axially uniform fields for use in electron paramagnetic resonance. II. Free space generalization, *Rev. Sci. Instrum.* **73**, 3027 (2002).
- [18] J. S. Hyde, R. R. Mett, and J. R. Anderson, Cavities with axially uniform fields for use in electron paramagnetic resonance. III. Re-entrant geometries, *Rev. Sci. Instrum.* **73**, 4003 (2002).
- [19] L. Krauss, J. Moody, F. Wilczek, and D. E. Morris, Calculations for cosmic axion detection, *Phys. Rev. Lett.* **55**, 1797 (1985).
- [20] W. U. Wuensch, S. De Panfilis-Wuensch, Y. K. Semertzidis, J. T. Rogers, A. C. Melissinos, H. J. Halama, B. E. Moskowitz, A. G. Prodell, W. B. Fowler, and F. A. Nezrick, Results of a laboratory search for cosmic axions and other weakly coupled light particles, *Phys. Rev. D* **40**, 3153 (1989).
- [21] R. Bradley, J. Clarke, D. Kinion, L. J. Rosenberg, K. van Bibber, S. Matsuki, M. Mück, and P. Sikivie, Microwave cavity searches for dark-matter axions, *Rev. Mod. Phys.* **75**, 777 (2003).
- [22] S. Asztalos, E. Daw, H. Peng, L. J. Rosenberg, C. Hagmann, D. Kinion, W. Stoeffl, K. van Bibber, P. Sikivie, N. S. Sullivan, D. B. Tanner, F. Nezrick, M. S. Turner, D. M. Moltz, J. Powell, M.-O. André, J. Clarke, M. Mück, and R. F. Bradley, Large-scale microwave cavity search for dark-matter axions, *Phys. Rev. D* **64**, 092003 (2001).
- [23] I. Stern, G. Carosi, N. Sullivan, and D. Tanner, Avoided Mode Crossings in Cylindrical Microwave Cavities, *Phys. Rev. Appl.* **12**, 044016 (2019).
- [24] T. A. Dyson, C. L. Bartram, A. Davidson, J. B. Ezekiel, L. M. Futamura, T. Liu, and C.-L. Kuo, High-volume tunable resonator for axion searches above 7 ghz, *Phys. Rev. Appl.* **21**, L041002 (2024).
- [25] C.-L. Kuo, Large-volume centimeter-wave cavities for axion searches, *J. Cosmol. Astropart. Phys.* **2020** (06), 010.
- [26] E. A. J. Marcatili, Dielectric rectangular waveguide and directional coupler for integrated optics, *Bell Syst. Tech. J.* **48**, 2071 (1969).
- [27] A. Kumar, A. Majumder, S. Chatterjee, S. Das, and S. Kar, A novel approach to determine the plasma frequency for wire media, *Metamaterials* **6**, 43 (2012).
- [28] B. T. McAllister, A. P. Quiskamp, and M. E. Tobar, Tunable rectangular resonant cavities for axion haloscopes, *Phys. Rev. D* **109**, 015013 (2024).